

# Schwarzschild black hole lensing

K. S. Virbhadra\* and George F. R. Ellis†

*Department of Applied Mathematics, University of Cape Town, Rondebosch 7701, South Africa*

We study strong gravitational lensing due to a Schwarzschild black hole. Apart from the primary and the secondary images we find a sequence of images on both sides of the optic axis; we call them *relativistic images*. These images are formed due to large bending of light near  $r = 3M$  (the closest distance of approach  $r_o$  is greater than  $3M$ ). The sources of the entire universe are mapped in the vicinity of the black hole by these images. For the case of the Galactic supermassive “black hole” they are formed at about 17 microarcseconds from the optic axis. The relativistic images are not resolved among themselves, but they are resolved from the primary and secondary images. However the relativistic images are very much demagnified unless the observer, lens and source are very highly aligned. Due to this and some other difficulties the observation of these images does not seem to be feasible in near future. However, it would be a great success of the general theory of relativity in a strong gravitational field if they ever were observed and it would also give an upper bound,  $r_o = 3.21M$ , to the compactness of the lens, which would support the black hole interpretation of the lensing object.

## I. INTRODUCTION

The phenomena resulting from the deflection of electromagnetic radiation in a gravitational field are referred to as *gravitational lensing* (GL) and an object causing a detectable deflection is known as a *gravitational lens*. The basic theory of GL was developed by Liebes [1], Refsdal [2], and Bourossa and Kantowski [3]. For detailed discussions on GL see the monograph by Schneider *et al.* [4] and reviews by Blandford and Narayan [5], Refsdal and Surdej [6], Narayan and Bartelmann [7] and Wambsganss [8].

The discovery of quasars in 1963 paved the way for observing point source GL. Walsh, Carswell and Weymann [9] discovered the first example of GL. They observed twin images QSO 0957+561 A,B separated by 5.7 arcseconds at the same redshift  $z_s = 1.405$  and  $\text{mag} \approx 17$ . Following this remarkable discovery more than a dozen convincing multiple-imaged quasars are known.

The vision of Zwicky that galaxies can be lensed was crystallized when Lynds and Petrosian [10] and Soucail *et al.* [11] independently observed giant blue luminous *arcs* of about 20 arcseconds long in the rich clusters of galaxies. Paczyński [12] interpreted these giant arcs to be distorted images of distant galaxies located behind the clusters. About 20 giant arcs have been observed in the rich clusters. Apart from the giant arcs, there have been also observed weakly distorted *arclets* which are images of other faint background galaxies [13].

Hewitt *et al.* [14] observed the first Einstein ring MG1131+0456 at redshift  $z_s = 1.13$ . With high resolution radio observations, they found the extended radio source to actually be a ring of diameter about 1.75 *arcseconds*. There are about half a dozen observed rings of diameters between 0.33 to 2 arcseconds and all of them are found in the radio waveband; some have optical and infrared counterparts as well [8].

The general theory of relativity has passed experimental tests in a weak gravitational field with flying colors; however, the theory has not been tested in a strong gravitational field. Testing the gravitational field in the vicinity of a compact massive object, such as a black hole or a neutron star, could be a possible avenue for such investigations. Dynamical observations of several galaxies show that their centres contain massive dark objects. Though there is no iron-clad evidence, indirect arguments suggest that these are supermassive black holes; at least, the case for black holes in the Galaxy as well as in NGC4258 appears to be strong [15]. These could be possible observational targets to test the Einstein theory of relativity in a strong gravitational field through GL.

Immediately after the advent of the general theory of relativity, Schwarzschild obtained a static spherically symmetric asymptotically flat vacuum solution to the Einstein equations, which was later found to have an event horizon when maximally extended; thus this solution represents the gravitational field of a spherically symmetric black hole

---

\*Email address : shwetket@maths.uct.ac.za

†Email address : ellis@maths.uct.ac.za

(see in Hawking and Ellis [16]). Schwarzschild GL in the weak gravitational field region (for which the deflection angle is small) is well-known [4]. Recently Kling *et al.* [17] developed an iterative approach to GL theory based on approximate solutions of the null geodesics equations, and to illustrate their method they constructed the iterative lens equations and time of arrival equation for a single Schwarzschild lens. In this paper we obtain a lens equation that allows for the large bending of light near a black hole, model the Galactic supermassive “black hole” as a Schwarzschild lens and study point source lensing in the strong gravitational field region, when the bending angle can be very large. Apart from a primary image and a secondary image (which are observed due to small bending of light in a weak gravitational field) we get a theoretically infinite sequence of images on both sides close to the optic axis; we term them *relativistic images*. The relativistic images are formed due to large bending of light in a strong gravitational field in the vicinity of  $3M$ , and are usually greatly demagnified (the magnification decreases very fast with an increase in the angular position of the source from the optic axis). Though the observation of relativistic images is a very difficult task (it is very unlikely that they will be observed in near future), if it ever were accomplished it would support the general theory of relativity in a strong gravitational field inaccessible to test the theory in any other known way and would also give an upper bound to the compactness of the lens. This is the subject of study in this paper. We use geometrized units (the gravitational constant  $G = 1$  and the speed of light in vacuum  $c = 1$  so that  $M \equiv MG/c^2$ ).

## II. LENS EQUATION, MAGNIFICATION AND CRITICAL CURVES

In this section we derive a lens equation that allows for the large bending of light near a black hole. The lens diagram is given in Fig.1. The line joining the observer  $O$  and the lens  $L$  is taken as the reference (optic) axis. The spacetime under consideration, with the lens (deflector) causing strong curvature, is asymptotically flat; the observer as well as the source are situated in the flat spacetime region (which can be embedded in an expanding Robertson-Walker universe).

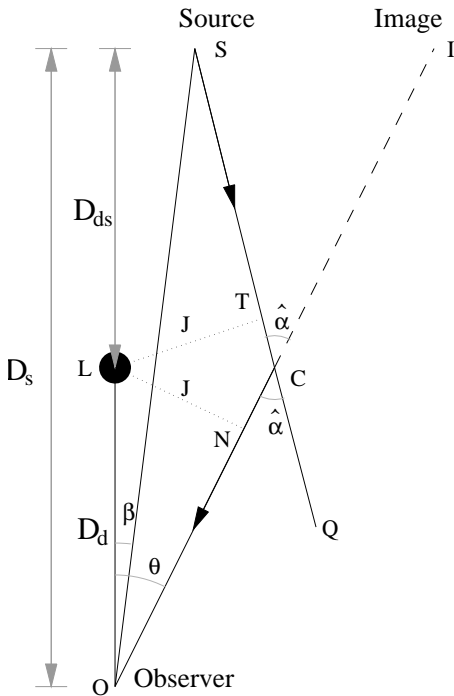


FIG. 1. The lens diagram:  $O, L$  and  $S$  are respectively the positions of the observer, deflector (lens) and source.  $OL$  is the reference (optic) axis.  $\angle LOS$  and  $\angle LOI$  are the angular separations of the source and the image from the optic axis.  $SQ$  and  $OI$  are respectively tangents to the null geodesic at the source and observer positions;  $LN$  and  $LT$ , the perpendiculars to these tangents from  $L$ , are the impact parameter  $J$ .  $\angle OCQ$ , is the Einstein bending angle.  $D_s$  represents the observer-source distance,  $D_{ds}$  the lens-source distance and  $D_d$  the observer-lens distance.

$SQ$  and  $OI$  are tangents to the null geodesic at the source and image positions, respectively;  $C$  is where their point of intersection would be if there were no lensing object present. The angular positions of the source and the image are measured from the optic axis  $OL$ .  $\angle LOI$  (denoted by  $\theta$ ) is the image position and  $\angle LOS$  (denoted by  $\beta$ ) is the source position if there were no lensing object.  $\hat{\alpha}$  (i.e.  $\angle OCQ$ ) is the Einstein deflection angle. The null geodesic and the

background broken geodesic path  $OCS$  will be almost identical, except near the lens where most of bending will take place. Given the vast distances from observer to lens and from lens to source, this will be a good approximation, even if the light goes round and round the lens before reaching the observer. We assume that the line joining the point  $C$  and the location of the lens  $L$  is perpendicular to the optic axis. This is a good approximation for small values of  $\beta$ . We draw perpendiculars  $LT$  and  $LN$  from  $L$  on the tangents  $SQ$  and  $OI$  respectively and these represent the impact parameter  $J$ .  $D_s$  and  $D_d$  stand for the distances of the source and the lens from the observer, and  $D_{ds}$  represents the lens-source distance, as shown in the Fig. 1. Thus, the lens equation may be expressed as

$$\tan \beta = \tan \theta - \alpha, \quad (1)$$

where

$$\alpha \equiv \frac{D_{ds}}{D_s} [\tan \theta + \tan (\hat{\alpha} - \theta)]. \quad (2)$$

The lens diagram gives

$$\sin \theta = \frac{J}{D_d}. \quad (3)$$

A gravitational field deflects a light ray and causes a change in the cross-section of a bundle of rays. The magnification of an image is defined as the ratio of the flux of the image to the flux of the unlensed source. According to Liouville's theorem the surface brightness is preserved in gravitational light deflection. Thus, the magnification of an image turns out to be the ratio of the solid angles of the image and of the unlensed source (at the observer). Therefore, for a circularly symmetric GL, the magnification of an image is given by

$$\mu = \left( \frac{\sin \beta}{\sin \theta} \frac{d\beta}{d\theta} \right)^{-1}. \quad (4)$$

The sign of the magnification of an image gives the parity of the image. The singularities in the magnification in the lens plane are known as *critical curves* (CCs) and the corresponding values in the source plane are known as *caustics*. Critical images are defined as images of 0-parity.

The tangential and radial magnifications are expressed by

$$\mu_t \equiv \left( \frac{\sin \beta}{\sin \theta} \right)^{-1}, \quad \mu_r \equiv \left( \frac{d\beta}{d\theta} \right)^{-1} \quad (5)$$

and singularities in these give *tangential critical curves* (TCCs) and *radial critical curves* (RCCs), respectively; the corresponding values in the source plane are known as *tangential caustic* (TC) and *radial caustics* (RCs), respectively. Obviously,  $\beta = 0$  gives the TC and the corresponding values of  $\theta$  are the TCCs. For small values of angles  $\beta$ ,  $\theta$  and  $\hat{\alpha}$  equations (1) and (4) yield the approximate lens equation and magnification, respectively, which have been widely used in studying lensing in a weak gravitational field [4].

### III. SCHWARZSCHILD SPACETIME AND THE DEFLECTION ANGLE

The Schwarzschild spacetime is expressed by the line element

$$ds^2 = \left(1 - \frac{2M}{r}\right) dt^2 - \left(1 - \frac{2M}{r}\right)^{-1} dr^2 - r^2 (d\vartheta^2 + \sin^2 \vartheta d\phi^2), \quad (6)$$

where  $M$  is the Schwarzschild mass. When this solution is maximally extended it has an event horizon at the Schwarzschild radius  $R_s = 2M$ . The deflection angle  $\hat{\alpha}$  for a light ray with closest distance of approach  $r_o$  is (Chapters 8.4 and 8.5 in [18])

$$\hat{\alpha}(r_o) = 2 \int_{r_o}^{\infty} \frac{dr}{r \sqrt{\left(\frac{r}{r_o}\right)^2 \left(1 - \frac{2M}{r_o}\right) - \left(1 - \frac{2M}{r}\right)}} - \pi \quad (7)$$

and the impact parameter  $J$  is

$$J = r_o \left(1 - \frac{2M}{r_o}\right)^{-\frac{1}{2}}. \quad (8)$$

A timelike hypersurface  $\{r = r_o\}$  in a spacetime is defined as a photon sphere if the Einstein bending angle of a light ray with the closest distance of approach  $r_0$  becomes unboundedly large. For the Schwarzschild metric  $r_0 = 3M$  is the photon sphere and thus the deflection angle  $\hat{\alpha}$  is finite for  $r_0 > 3M$ .

The Einstein deflection angle for large  $r_o$  is [19]

$$\hat{\alpha}(r_o) = \frac{4M}{r_o} + \frac{4M^2}{r_o^2} \left(\frac{15\pi}{16} - 1\right) + \dots \quad (9)$$

We mentioned the above result only for completeness as it is not much known in the literature. As we are interested to study GL due to light deflection in a strong gravitational field we will use Eq. (7) for any further calculations. Introducing radial distance defined in terms of the Schwarzschild radius,

$$x = \frac{r}{2M}, \quad x_o = \frac{r_o}{2M}, \quad (10)$$

the deflection angle  $\hat{\alpha}$  and the impact parameter  $J$  take the form

$$\hat{\alpha}(x_o) = 2 \int_{x_o}^{\infty} \frac{dx}{x \sqrt{\left(\frac{x}{x_o}\right)^2 \left(1 - \frac{1}{x_o}\right) - \left(1 - \frac{1}{x}\right)}} - \pi \quad (11)$$

and

$$J = 2Mx_o \left(1 - \frac{1}{x_o}\right)^{-\frac{1}{2}}. \quad (12)$$

In the computations in the following section we require the first derivative of the deflection angle  $\hat{\alpha}$  with respect to  $\theta$ . This is given by (see in [19])

$$\frac{d\hat{\alpha}}{d\theta} = \hat{\alpha}'(x_o) \frac{dx_o}{d\theta}, \quad (13)$$

where

$$\frac{dx_o}{d\theta} = \frac{x_o \left(1 - \frac{1}{x_o}\right)^{\frac{3}{2}} \sqrt{1 - \left(\frac{2M}{D_d}\right)^2 x_o^2 \left(1 - \frac{1}{x_o}\right)^{-1}}}{\frac{M}{D_d} (2x_o - 3)} \quad (14)$$

and the first derivative of  $\hat{\alpha}$  with respect to  $x_o$  is

$$\hat{\alpha}'(x_o) = \frac{3 - 2x_o}{x_o^2 \left(1 - \frac{1}{x_o}\right)} \int_{x_o}^{\infty} \frac{(4x - 3) dx}{(3 - 2x)^2 x \sqrt{\left(\frac{x}{x_o}\right)^2 \left(1 - \frac{1}{x_o}\right) - \left(1 - \frac{1}{x}\right)}}. \quad (15)$$

#### IV. LENSING WITH THE GALACTIC SUPERMASSIVE “BLACK HOLE”

It is known that the Schwarzschild GL in a weak gravitational field gives rise to an Einstein ring when the source, lens and observer are aligned, and a pair of images (primary and secondary) of opposite parities when the lens components are misaligned. However, when the lens is a massive compact object a strong gravitational field is “available” for investigation. A light ray can pass close to the photon sphere and go around the lens once, twice, thrice, or many times (depending on the impact parameter  $J$  but for  $J > 3\sqrt{3}M$ ) before reaching the observer. Thus, a massive compact lens gives rise, in addition to the primary and secondary images, to a large number (indeed, theoretically an infinite sequence) of images on both sides of the optic axis. We call these images (which are formed due to the bending of light through more than  $3\pi/2$ ) *relativistic images*, as the light rays giving rise to them pass through a

strong gravitational field before reaching the observer. We call the rings which are formed by bending of light rays more than  $2\pi$ , *relativistic Einstein rings*.

We model the Galactic supermassive “black hole” as a Schwarzschild lens. This has mass  $M = 2.8 \times 10^6 M_\odot$  and the distance  $D_d = 8.5 \text{ kpc}$  [15]; therefore, the ratio of the mass to the distance  $M/D_d \approx 1.57 \times 10^{-11}$ . We consider a point source, with the lens situated half way between the source and the observer, i.e.  $D_{ds}/D_s = 1/2$ . We allow the angular position of the source to change keeping  $D_{ds}$  fixed.

We compute positions and magnifications of two pairs of outermost relativistic images as well as the primary and secondary images for different values of the angular positions of the source. These are shown in figures 2 and 3 and Table 1 (for relativistic images) and in Fig. 4 and Table 2 (for primary and secondary images). The angular positions of the primary and secondary images as well as the critical curves are given in arcseconds; those for relativistic images as well as relativistic critical curves are expressed in microarcseconds.

In Fig.2 we show how the positions of outer two relativistic images on each side of the optic axis change as the source position changes. To find the angular positions of images on the same side of the source we plot  $\alpha$  (represented by continuous curves on right side of the figure) and  $\tan \theta - \tan \beta$  (represented by dashed curves) against  $\theta$  for a given value of the source position  $\beta$ ; the points of intersection give the image positions (see the right side of the Fig. 3).

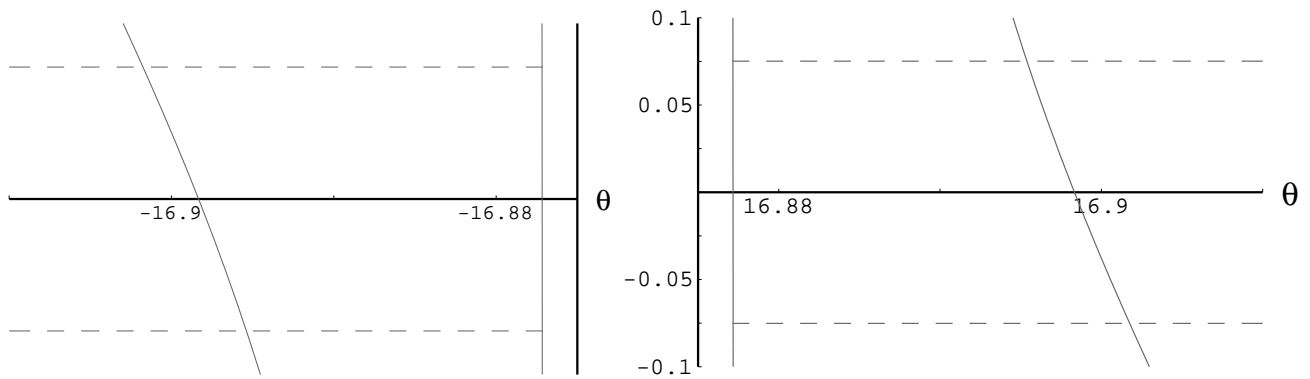


FIG. 2. This gives relativistic image positions for a given source position.  $\alpha$  and  $\tan \theta - \tan \beta$  are plotted against the angular position  $\theta$  of the image; these are represented by the continuous and the dashed curves, respectively. For a given position of the source, the points of intersections of the continuous curves (the two outermost ones on each side being shown) with the dashed curves give the angular positions of relativistic images. The Galactic “black hole” (mass  $M = 2.8 \times 10^6 M_\odot$  and the distance  $D_d = 8.5 \text{ kpc}$  so that  $M/D_d \approx 1.57 \times 10^{-11}$ ) serves as the lens,  $D_{ds}/D_s = 1/2$ , and  $\beta = \mp 0.075$  radian ( $\approx \mp 4.29718^\circ$ ).  $\theta$  is expressed in microarcseconds. The angular position of a relativistic image changes very slowly with respect to a change in the source position.

TABLE I. Magnifications and positions<sup>c</sup> of relativistic images

Images on the opposite side of the source		Source position $\beta$	Images on the same side of the source	
$\mu^{outer}$	$\mu^{inner}$		$\mu^{inner}$	$\mu^{outer}$
$-3.5 \times 10^{-12}$	$-6.5 \times 10^{-15}$	1	$6.5 \times 10^{-15}$	$3.5 \times 10^{-12}$
$-3.5 \times 10^{-13}$	$-6.5 \times 10^{-16}$	10	$6.5 \times 10^{-16}$	$3.5 \times 10^{-13}$
$-3.5 \times 10^{-14}$	$-6.5 \times 10^{-17}$	$10^2$	$6.5 \times 10^{-17}$	$3.5 \times 10^{-14}$
$-3.5 \times 10^{-15}$	$-6.5 \times 10^{-18}$	$10^3$	$6.5 \times 10^{-18}$	$3.5 \times 10^{-15}$
$-3.5 \times 10^{-16}$	$-6.5 \times 10^{-19}$	$10^4$	$6.5 \times 10^{-19}$	$3.5 \times 10^{-16}$
$-3.5 \times 10^{-17}$	$-6.5 \times 10^{-20}$	$10^5$	$6.5 \times 10^{-20}$	$3.5 \times 10^{-17}$
$-3.5 \times 10^{-18}$	$-6.5 \times 10^{-21}$	$10^6$	$6.5 \times 10^{-21}$	$3.5 \times 10^{-18}$

<sup>a</sup> The lens is the Galactic “black hole” (mass  $M = 2.8 \times 10^6 M_\odot$  and the distance  $D_d = 8.5 \text{ kpc}$  so that  $M/D_d \approx 1.57 \times 10^{-11}$ ). The ratio of the lens-source distance  $D_{ds}$  to the observer-source distance  $D_s$  is taken to be  $1/2$ . Angles are given in microarcseconds.

<sup>b</sup>  $\mu$  is the magnification and the sign on this refers to the parity of the image.

<sup>c</sup> For the source positions considered here, the angular positions of two pairs of outermost relativistic images are  $\approx \pm 16.898$  and  $\approx \pm 16.877$  microarcseconds ( + sign refers to images on the same side of the source and – sign refers to images on opposite side of the source).

Similarly, we plot  $-\alpha$  and  $-\tan\theta - \tan\beta$  vs.  $-\theta$  and points of intersection give the image positions on the opposite side of the source (see left side of the Fig. 2). We have taken  $\beta = \mp 0.075$  radian ( $\approx \mp 4.29718^\circ$ ). In fact there are a sequence of theoretically an infinite number of continuous curves which intersect with a given dashed curve giving rise to a sequence of an infinite number of images on both sides of the optic axis. We have plotted only two sets of such curves (note that the third set of continuous curves comes to be very close to the second set and therefore it is not possible to show them in the same figure) demonstrating appearance of two relativistic images on both sides of the optic axis. For  $\beta = 0$  the points of intersection of the continuous curves with the dashed curve give a sequence of infinite number of relativistic tangential critical curves (relativistic Einstein rings). As  $\beta$  increases any image on the same side of source moves away from the optic axis, whereas any image on the opposite side of the source moves towards the optic axis. The displacement of relativistic images with respect to a change in the source position is very small (see Fig. 2). The two sets of outermost relativistic images are formed at about 17 microarcseconds from the optic axis.

In Fig. 3 we plot the tangential magnification  $\mu_t$  as well as the total magnification  $\mu$  vs. the image position  $\theta$  near the two outermost relativistic tangential critical curves. The singularities in  $\mu_t$  give the angular radii of the two relativistic Einstein rings. In Fig. 4 we plot the same for the primary-secondary images; the singularity in  $\mu_t$  gives the angular position of the Einstein ring. The magnification for relativistic images falls extremely fast (as compared with the case of primary and secondary images) as the source position increases from perfect alignment. The tangential parity (sign of  $\mu_t$ ) as well as the total parity (sign of  $\mu$ ) are positive for all images on the same side of the source and negative for all images on the opposite side of the source. The radial parity (sign of  $\mu_r$ ) is positive for all the images in Schwarzschild lensing.

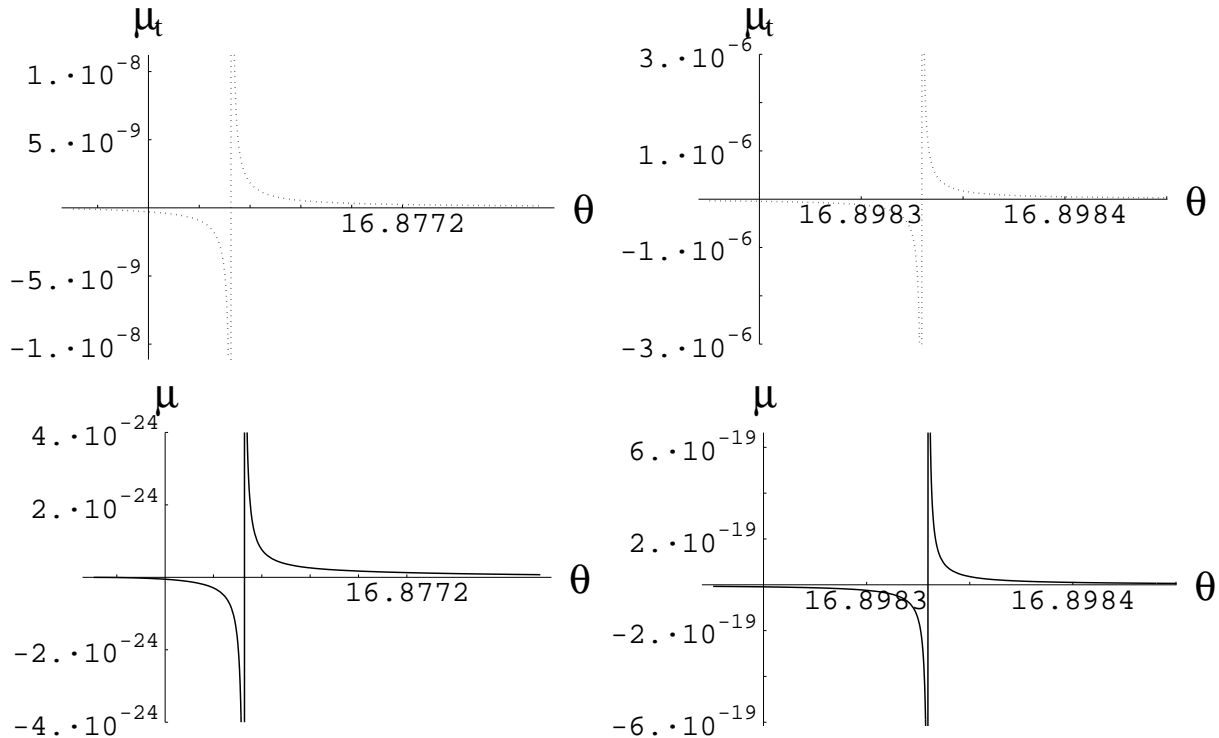


FIG. 3. The *tangential magnification*  $\mu_t$  denoted by dotted curves and the *total magnification*  $\mu$  denoted by continuous curves are plotted against the image position (expressed in microarcseconds) near relativistic tangential critical curves. The figures on the right side give the magnification for the outermost relativistic image, whereas those on left side are for a relativistic image adjacent to the previous one. The lens is the Galactic “black hole” ( $M/D_d \approx 1.57 \times 10^{-11}$ ) and  $D_{ds}/D_s = 1/2$ . The singularities in magnifications show the angular positions of the relativistic tangential critical curves. The origin of the  $\theta$ -axis for the figures on the left side is 16.87715 and for each on right side is 16.89825.

TABLE II. Positions and magnifications of primary and secondary images

Secondary images		Source position $\beta$	Primary images	
$\theta$	$\mu$		$\theta$	$\mu$
1.157494	-5787.20	$10^{-4}$	1.157594	5788.21
1.157045	-578.27	$10^{-3}$	1.158045	579.27
1.152555	-57.38	$10^{-2}$	1.162555	58.38
1.108619	-5.30	$10^{-1}$	1.208624	6.30
0.760918	-0.23	1	1.760914	1.23
0.529680	-0.05	2	2.529674	1.05
0.394711	-0.01	3	3.394704	1.01
0.310831	-0.005	4	4.310823	1.005
0.254986	-0.002	5	5.254977	1.002

<sup>a</sup> The same as in Table 1, except angles are given here in arcseconds.

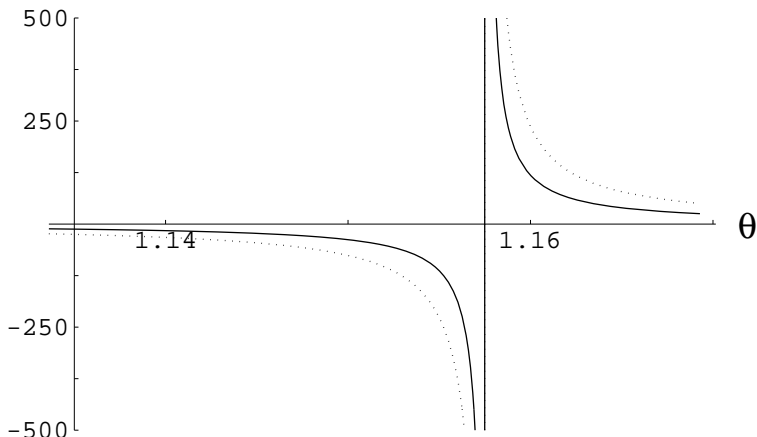


FIG. 4. The *tangential magnification*  $\mu_t$  (represented by dotted curves) and the *total magnification*  $\mu$  (represented by continuous curves) are plotted, near the outermost tangential critical curve, as a function of the image position (in arcseconds). The singularity gives the position of the outermost tangential critical curve (angular radius of the Einstein ring). The Galactic “black hole” is the lens and  $D_{ds}/D_s$  is taken to be  $1/2$ .

TABLE III. Einstein and relativistic Einstein rings

Rings	$\theta_E$	$\hat{\alpha}$	$\frac{r_o}{2M}$
Einstein ring	1.157544 <i>arcsec</i>	2.315089 <i>arcsec</i>	178193
Relativistic Einstein ring I	16.898 $\mu as$	$2\pi + 33.80 \mu as$	1.545115
Relativistic Einstein ring II	16.877 $\mu as$	$4\pi + 33.75 \mu as$	1.501875

<sup>a</sup> The same as (a) of Table 1, except *arcsec* and  $\mu as$  used here refer to arcseconds and microarcseconds, respectively.  $\theta_E$  stands for the angular positions of tangential critical curves.

In Table 3 we give the angular radii  $\theta_E$  of the Einstein and two relativistic Einstein rings. We also give the corresponding values for the deflection angle  $\hat{\alpha}$  and the closest distance of approach  $x_o$  for the light rays giving rise to these rings. We define an “effective deflection angle”  $\hat{\alpha} - 2\pi$  times the number of revolution the light ray has made before reaching the observer. Table 3 shows that the effective deflection angle for a ring decreases with the decrease in its angular radius, which is expected from the geometry of the lens diagram. The same is true for images on the same side of the optic axis, i.e. the effective deflection angle is less for images closer to the optic axis.

The supermassive “black holes” at the centres of *NGC3115* and *NGC4486* have  $M/D_d \approx 1.14 \times 10^{-11}$  and  $1.03 \times 10^{-11}$ , respectively [15], which are very close to the case of the Galactic “black hole” we have studied. Therefore, if we study lensing with these “black holes” keeping  $D_{ds}/D_s = 1/2$ , we will get approximately the same results. The angular radius of the Einstein ring in the Schwarzschild lensing is expressed by  $\theta_E = \{4MD_{ds}/(D_dD_s)\}^{1/2}$ . For a source with  $D_{ds} < D_s$  one has  $0 < (D_{ds}/D_s) < 1$ . If we consider  $D_{ds}/D_s$  different than  $1/2$  the magnitude of the Einstein ring can easily be estimated. As relativistic images are formed due to light deflection close to  $r_o = 3M$ , their angular positions will be very much less sensitive to a change in the value of  $D_{ds}/D_s$ . We have considered the sources for  $D_d < D_s$ ; however, sources with  $D_d > D_s$  will also be lensed and will also give rise to relativistic images. Thus, all the sources of the universe will be mapped as relativistic images in the vicinity of the black hole (albeit as very faint images). Gravitational lensing with stellar-mass black holes will also give rise to relativistic images; however, unlike in the case of supermassive “black hole” lensing, these images will not be resolved from their primary and secondary images with present observational facilities.

## V. RELATIVISTIC IMAGES AS TEST FOR GENERAL RELATIVITY IN STRONG GRAVITATIONAL FIELD

For the Galactic “black hole” lens, Fig. 2 and Table 1 (see caption (c) ) show the angular positions of the two outermost sets of relativistic images (two images on each side of the optic axis) when a source position is given. In fact, there is a sequence of a large number of relativistic Einstein rings when the source, lens and observer are perfectly aligned, and when the alignment is “broken” there is a sequence of large number of relativistic images on both sides of the optic axis. However, for a given source position their magnifications decrease very fast as the angular position  $\theta$  decreases (see Table 1), and therefore the outermost set of images, one on each side of the optic axis, is observationally the most significant. The angular separations among relativistic images are too small to be resolved with presently available instruments and therefore all these images would be at the same position; however, these relativistic images will be resolved from the primary and secondary images and thus resolution is not a problem for observation of relativistic images.

If we observe a full or “broken” Einstein ring near the centre of a massive dark object at the centre of a galaxy with a faint relativistic image of the same source at the centre of the ring, we would expect that the central (relativistic) image would disappear after a short period of time. If seen, this would be a great success of the general theory of relativity in a strong gravitational field.

Observation of relativistic images would also give an upper bound on the compactness of the lens. To get a relativistic image a light ray has to suffer a deflection by an angle  $\hat{\alpha} > 3\pi/2$ . For the closest distance of approach  $r_o = 3.208532M$  the deflection angle  $\hat{\alpha} = 269.9999^\circ$  and therefore  $r_o/M = 3.208532$  can be considered as an upper bound to the compactness of the lens. The fact that the magnification of a relativistic image decreases very fast as the source position increases from its perfect alignment with the lens and observer can be exploited to give a better estimate of the compactness of the lens. For the lens system considered in section four, the outermost relativistic Einstein ring has angular radius about 16.898 microarcseconds and this is formed due to light rays bending at the closest distance of approach  $r_o \approx 3.09023M_\odot$  (see Table 3). As a relativistic image can be observed only very close to a relativistic TCC, the above value of the  $r_o/M$  gives an estimate of compactness of the massive dark object.

There are some serious difficulties hindering the observation of the primary-secondary image pair near a galactic centre; the observation of relativistic images is even much more difficult. The extinction of electromagnetic radiation near the line of sight to galactic nuclei would be appreciable; the smaller the wavelength, the larger the extinction. The interstellar scattering and radiation at several frequencies from the material accreting on the “black hole” would make these observations more difficult. Due to these obstacles no lensing event near a galactic centre has been observed till now, but it seems this is a very worthwhile project.

There are some additional difficulties for observing relativistic images. First, these images are very much demagnified unless the source, lens and observer are highly aligned. When the source position  $\beta$  decreases the magnification increases rapidly and therefore one may possibly get observable relativistic images, but only if the source, lens and observer are highly aligned ( $\beta \ll 1$  microarcsecond) and the source has a large surface brightness. Quasars and supernovae would be ideal sources for observations of relativistic images. The number of observed quasars is low (about  $10^4$ , see in [8]) and therefore the probability that a quasar will be highly aligned along the direction of any galactic centre of observed galaxies is extremely small. Similarly, there is a very small probability that a supernova will be strongly aligned with any galactic centre. We considered a normal star in the Galaxy to be a point source (note that we took  $D_{ds}/D_s = 1/2$ ). We cannot use the point source approximation when such a source is very close to the caustic ( $\beta = 0$ ) and therefore studies of extended source lensing are needed. Second, if relativistic images were observed it would be for a short period of time because the magnification decreases very fast with increase in the

source position; however, the time scale for observation of relativistic images will be greater for lensing of more distant sources. It is highly improbable that the relativistic images would in fact be observed in a short observing period and a long term project to search for such images would not have reasonable probability of success. Nevertheless the possibility remains that such images might be detected through lucky observations in the vicinity of galactic centers.

## VI. SUMMARY

We obtained a lens equation which allows an arbitrary large values of the deflection angle and used the deflection angle expression for the Schwarzschild metric obtained by Weinberg [18]. This gives the bending angle of a light ray passing through the Schwarzschild gravitational field for a closest distance of approach  $r_o$  in the range  $3M < r_o < \infty$ . Using this we studied GL due to the Galactic “black hole” in a strong gravitational field.

Apart from a pair of images (primary and secondary) which are observed due to light deflection in a weak gravitational field, we find a sequence of large number of relativistic images on both sides of the optic axis due to large deflections of light in a strong gravitational field near the photon sphere  $r_o = 3M$ . Among these relativistic images, the outermost pair is observationally the most important. Though these relativistic images are resolved from the primary and secondary images, there are serious difficulties in observing them. However, if it were to succeed it would be a great triumph of the general theory of relativity and would also provide valuable information about the nature of massive dark objects. Observations of relativistic images would confirm the Schwarzschild geometry close to the event horizon; therefore these would strongly support the black hole interpretation of the lensing object.

In the investigations in this paper we modelled the massive compact objects as Schwarzschild lens. However, it is worth investigating Kerr lensing to see the effect of rotation on lensing in strong gravitational field, especially when the lens has large intrinsic angular momentum to the mass ratio. There have been some studies of Kerr weak field lensing (see Rauch and Blandford [20] and references therein). In passing, it is worth mentioning that any spacetime endowed with a photon sphere (as defined in Section III) and acting as a gravitational lens would give rise to relativistic images.

## ACKNOWLEDGMENTS

Thanks are due to H. M. Antia, M. Dominik, J. Kormendy, J. Lehar, and D. Narasimha for helpful correspondence, and J. Menzies and P. Whitelock for helpful discussions on the visibility of images. This research was supported by FRD, S. Africa.

- 
- [1] Jr. S. Leibes, Phys. Rev. **133**, B835 (1964).
  - [2] S. Refsdal, Mon. Not. Roy. Soc. **128**, 295 (1964).
  - [3] R. R. Bourassa and R. Kantowski, Astrophys. J. **195**, 13 (1975).
  - [4] P. Schneider, J. Ehlers, and E. E. Falco, *Gravitational Lenses* (Springer Verlag, Berlin, 1992).
  - [5] R. D. Blandford and R. Narayan, Ann. Rev. Astron. Astrophys. **30**, 311 (1992).
  - [6] S. Refsdal and J. Surdej, Rep. Prog. Theor. Phys. **56**, 117 (1994).
  - [7] R. Narayan and M. Bartelmann, “Lectures on Gravitational Lensing,” astro-ph/9606001.
  - [8] J. Wambsganss, “Gravitational Lensing in Astronomy,” astro-ph/9812021.
  - [9] D. Walsh, R. F. Carswell, and R. J. Weymann, Nature **279**, 381 (1979).
  - [10] R. Lynds and V. Petrosian, Bull. Am. Astron. Soc. **18**, 1014 (1986).
  - [11] G. Soucail, B. Fort, Y. Mellier, and J. P. Picat, Astron. Astrophys. **172**, L14 (1987).
  - [12] B. Paczyński, Nature **325**, 572 (1987).
  - [13] J. A. Tyson, Astrophys. J. **96**, 1 (1988).
  - [14] J. N. Hewitt J. N. *et al.*, Nature **333**, 537 (1988).
  - [15] D. Richstone *et al.*, Nature **395**, A14 (1998).
  - [16] S. W. Hawking and G. F. R. Ellis, *The Large Scale Structure of Space-Time* (Cambridge University Press, Cambridge, England, 1973).
  - [17] T. P. Kling, E. T. Newman, and A. Perez, “Iterative Approach to Gravitational Lensing Theory,” gr-qc/9908082.

- [18] S. Weinberg, *Gravitation and Cosmology: Principles and Applications of the General Theory of Relativity* (Wiley, New York, 1972).
- [19] K. S. Virbhadra, D. Narasimha, and S. M. Chitre, *Astron. Astrophys.* **337**, 1 (1998).
- [20] K. P. Rauch and R. D. Blandford, *Astrophys. J.* **421**, 46 (1994).